

Finite-size effects on transverse magnetoresistance of NbSe₃

Yamaguchi Takahide, Shinya Uji, Kengo Enomoto, Takako Konoike, Taichi Terashima, and Mitsuka Nishimura
National Institute for Materials Science, Tsukuba 305-0003, Japan

Taku Tsuneta, Katsuhiko Inagaki, Satoshi Tanda, and Kazuhiko Yamaya
Graduate School of Engineering, Hokkaido University, Sapporo 060-8628, Japan
 (Received 17 November 2004; published 12 April 2005)

A charge-density-wave material NbSe₃ with thickness less than 1 μm shows a distinct peak in the low temperature transverse magnetoresistance when the magnetic field is applied along the *c* axis. The resistance peak is less pronounced as the field is tilted away from the *c* axis to the *a*^{*} axis. The peak height also decreases as the temperature increases, although the magnetic field at the peak shows no appreciable dependence on temperature. The resistance peak is attributed to surface diffuse scattering of normal carriers which remain even below the lower charge-density-wave transition temperature.

DOI: 10.1103/PhysRevB.71.134409

PACS number(s): 75.70.-i, 72.15.Nj, 73.23.-b, 71.45.Lr

Niobium triselenide (NbSe₃) is a quasi-one-dimensional conductor having a ribbon shape which extends along the *b* axis and has the wider transverse dimension along the *c* axis. It exhibits two charge-density-wave (CDW) transitions at $T_1=144$ K and $T_2=59$ K, but remains metallic at $T < T_2$.¹ It has a large electric conductivity along the *b* axis even under the electric field *E* lower than the threshold E_T for the CDW sliding. Below about 10 K, the magnetoresistance exhibits the Shubnikov-de Haas (SdH) oscillation. Extensive studies on the SdH oscillation for different orientations of the magnetic field have shown that there exist small pockets of the Fermi surface in the shape of nearly an ellipsoid, indicating that the nesting of the Fermi surface is imperfect.²⁻⁶

Recently, interesting features in NbSe₃ crystals with reduced cross sections have been reported. The threshold electric field E_T increases with decreasing thickness and/or width of the NbSe₃ crystals.^{7,8} It is also found that the resistance ratio $R(300\text{ K})/R(4.2\text{ K})$ decreases rapidly with decreasing thickness below about 1 μm, which is attributed to the surface scattering of normal carriers at the low temperature.⁷ Measurements⁹ on NbSe₃ crystals with cross-sectional areas reduced to 1 μm² by a plasma-etching process show that the phase slip voltage¹⁰ significantly decreases when the spacing between current probes is smaller than a few μm. Furthermore, metal-oxide-semiconductor field-effect transistor (MOSFET) like devices are fabricated of very thin NbSe₃ crystals with a thickness of much less than 1 μm.¹¹ Despite the growing interest in electrical transport properties on NbSe₃ crystals with such small cross sections, systematic magnetoresistance measurements of them are still lacking.

In this study, we have measured the low-temperature transverse magnetoresistance of NbSe₃ crystals with a thickness of less than 1 μm and found that the magnetoresistance curves have a maximum at a low magnetic field ($B < 1$ T) in addition to the SdH oscillation at $B \geq 2$ T. We show that the resistance maximum is attributed to the finite-size effect on the ballistic transport of the normal carriers, namely, their surface diffuse scattering.

NbSe₃ crystals are placed on silicon substrates and more than four gold wires are attached to a crystal by silver paste.

We took a great care in selecting crystals with well defined facets using an optical microscope. Typical crystal dimensions are 0.2–0.6 μm along the *a*^{*} axis, 1–3 μm along the *c* axis, and a few millimeters along the *b* axis. The crystal dimensions are described in Table I. We measured the resistance using a standard ac lock-in technique with a small excitation current so that $E < E_T$. The samples were cooled down by a ³He or a ⁴He refrigerator equipped with a superconducting magnet.

Figure 1 shows typical magnetoresistance curves for a thin crystal (1) measured at several temperatures. We can see the SdH oscillation at magnetic fields larger than about 2 T. The dominant frequency of the oscillation is 28 T for the magnetic field parallel to the *c* axis. The angular dependence of the oscillations was also measured, which showed that the frequency increases monotonically to 95 T as the orientation of the magnetic field is rotated away from the *c* axis towards *a*^{*}. The values of the frequency indicate that the maximum cross-sectional areas S_{a^*b} and S_{bc} of the Fermi surface in the *a*^{*}*b* and *bc* planes are 2.7×10^{17} m⁻² and 9.1×10^{17} m⁻², respectively. The angular dependence of the frequency, namely, that of the cross-sectional areas of the Fermi surface is approximately the same as that obtained by other groups.²⁻⁵ For $B // c$, the carrier effective mass m^* is estimated to be $0.20m_0$ (m_0 is the free electron mass), and the

TABLE I. Parameters of seven NbSe₃ crystals. d_{a^*} and d_c are the thickness along the *a*^{*} axis and the width along the *c* axis, respectively.

Sample	$d_{a^*}(\mu\text{m})$	$d_c(\mu\text{m})$	$R(300\text{ K})/R(4.2\text{ K})$
1	0.49	1.59	29
2	0.60	2.40	66
3	3.9	13.2	110
4	0.46	2.75	64
5	0.21	1.37	25
6	0.46	0.78	64
7	1.9	14.2	54

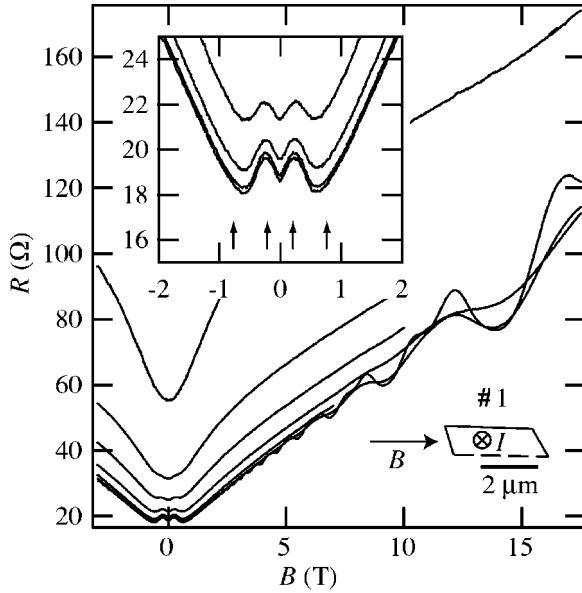


FIG. 1. The magnetoresistance of a NbSe₃ crystal with 0.49 μm thickness (sample 1) at several temperatures; $T=16.00$ K, 12.00 K, 10.00 K, 8.00 K, 6.00 K, 4.00 K, and 0.28 K from the top curve to the bottom one. Inset: An enlargement of the low-magnetic-field region. $T=8.00$ K, 6.00 K, 4.00 K, and 0.28 K from top to bottom. The arrows indicate the magnetic fields $B=0.55\hbar\sqrt{S_{a^*b^*}}/\pi/ed_{a^*}$ and $2.0\hbar\sqrt{S_{a^*b^*}}/\pi/ed_{a^*}$.

Dingle temperature T_D is 1.5 K. These values are comparable to m^* of $0.30m_0$ (Ref. 2) and $0.24m_0$ (Ref. 3) and to T_D of 1.7 K (Ref. 2) and 2.3 K (Ref. 3) in the literature. Besides the SdH oscillation at higher fields, there is a resistance maximum at a low field as shown in the inset of Fig. 1. The magnetic field B_{\max} , where the resistance is at its maximum, shows no appreciable dependence on temperature, although the zero-field resistance increases with increasing temperature.

Figure 2 shows magnetoresistance curves for two crystals with different cross-sectional areas, which are measured at the same time in the same cryostat. Two series of curves in each figure correspond to two different sets of voltage probes. The measured $R(B)$ curves, in particular of the thick sample (3), are not quite symmetric, most probably due to the inclusion of Hall resistance. To remove the component of the Hall resistance, we averaged the results for the two opposite polarities of the magnetic field. The $R(B)$ curves for sample 3 have no peak structure and are similar for different orientations of the magnetic field. On the other hand, the $R(B)$ curves of the thin crystal (4) have a clear maximum for magnetic-field directions close to the c axis. The peak structure becomes less evident as the field direction deviates from the c axis.

The resistance maximum can be explained by semiclassical theory treating surface diffuse scattering of carriers. Within the Boltzmann equation approach, MacDonald and Sarginson¹² calculated the transverse magnetoresistivity $\rho(B)$ of a metal film with $d/l \leq 1$ (d is film thickness, and l is the bulk mean free path) under the condition that both the current and the magnetic field are in the plane of the film. Their

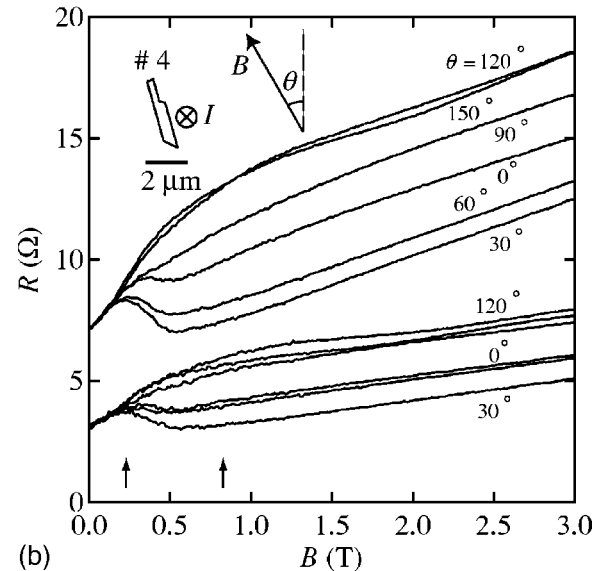
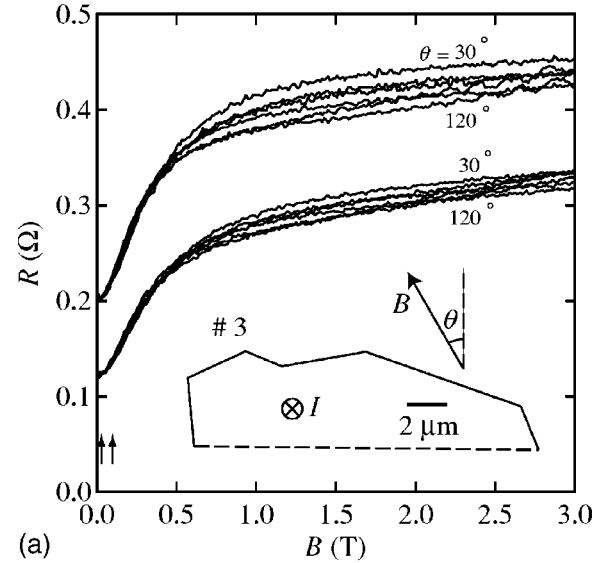


FIG. 2. The magnetoresistance of (a) thick (3) and (b) thin (4) crystals, measured at 0.28 K for the field orientations $\theta=0^\circ, 30^\circ, 60^\circ, 90^\circ, 120^\circ$, and 150° . The c axis corresponds to $\theta=98^\circ$ for sample 3 and $\theta=36^\circ$ for sample 4. The arrows indicate the magnetic fields $B=0.55\hbar\sqrt{S_{a^*b^*}}/\pi/ed_{a^*}$ and $2.0\hbar\sqrt{S_{a^*b^*}}/\pi/ed_{a^*}$.

calculation shows that the $\rho(B)$ curve has a maximum. At zero field, the resistivity is larger than the bulk resistivity because of the surface diffuse scattering. The resistivity increases with increasing field as the carrier orbit is bent by the Lorentz force and, consequently, the carriers are scattered more frequently at the edges. At larger fields where the diameter of the cyclotron orbit is smaller than d , the resistivity is close to the bulk value because the carriers do not reach the edges unless they suffer internal collisions. As expected intuitively, the maximum value of ρ/ρ_{bulk} is larger for smaller d/l . An improved calculation¹³ shows that $\rho(B)$ reaches the maximum when $d/r_C=0.55$, namely, $B=0.55\hbar k_F/ed$, irrespective of the ratio d/l . Here, r_C is the cyclotron radius and k_F is the Fermi wave number. It also shows that the $\rho(B)$ curve has a sharp bend at B

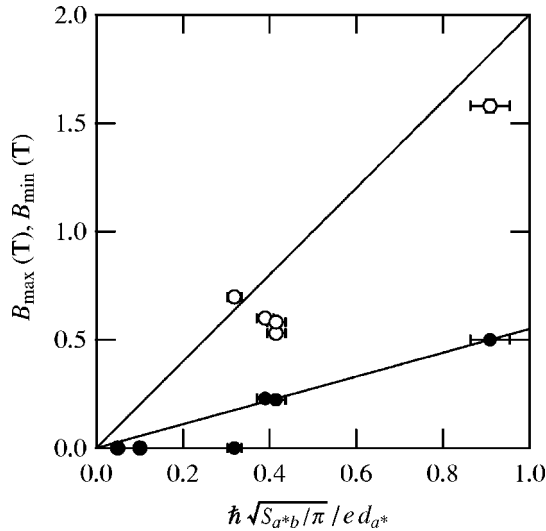


FIG. 3. The magnetic fields B_{\max} and B_{\min} , where the magnetoresistance curves show a maximum and a minimum, plotted as a function of $\hbar\sqrt{S_{a^*b}/\pi}/ed_{a^*}$. The closed and open circles show B_{\max} and B_{\min} , respectively. The solid lines have slopes of 0.55 and 2.0.

$=2.0\hbar k_F/ed$, above which the resistivity approaches the bulk value. Experimentally, such magnetoresistance peaks due to diffuse surface scattering of carriers have been observed in pure metal films¹⁴ and in narrow conducting channels of two-dimensional electron gas.¹⁵

To compare the experimental results with the theory, it is necessary to know the thicknesses d of the NbSe₃ crystals. We took pictures of the crystals by a scanning electron microscope (SEM), typically about 16 pictures for each sample, at different angles. The pictures were taken after the measurements to avoid possible damage caused by the electron beam. The nominal error in length scale of the SEM pictures is 10%. We plotted the widths of major facets seen in the pictures as a function of the angle, and fitted the data to cosine curves to determine the actual widths and directions of the facets. The cross-sectional profiles estimated in this way are depicted in the insets of Figs. 1 and 2, and 4. Some of the crystals do not have cross sections of simple parallelograms. For simplicity, we take the average thickness for such crystals.

The arrows in Figs. 1 and 2 indicate the magnetic fields $B=0.55\hbar\sqrt{S_{a^*b}/\pi}/ed_{a^*}$ and $2.0\hbar\sqrt{S_{a^*b}/\pi}/ed_{a^*}$, where d_{a^*} is the thickness in the a^* direction. The calculation in Ref. 13 assumes a spherical Fermi surface, but the Fermi surface of NbSe₃ is close to an ellipsoid in shape, as described above. Since it is a formidable task to perform a calculation similar to that in Ref. 13 by taking account of the shape of the Fermi surface, we approximate k_F as $\sqrt{S_{a^*b}/\pi}$ for $B//c$. One can see that the positions of the arrows are close to B_{\max} and B_{\min} , where the resistance is at its maximum and minimum. We plot B_{\max} and B_{\min} for seven crystals as a function of $\hbar\sqrt{S_{a^*b}/\pi}/ed_{a^*}$ in Fig. 3. The points for B_{\max} and B_{\min} lie approximately on the straight lines with slopes of 0.55 and 2.0, respectively. Note that the points showing $B_{\max}=0$ ($B_{\min}=0$) mean that the maximum (minimum) is not observed in the $R(B)$ curves of the crystals.

The absence of the resistance maximum and minimum for the thick samples, 3 and 7, suggests that the bulk mean free

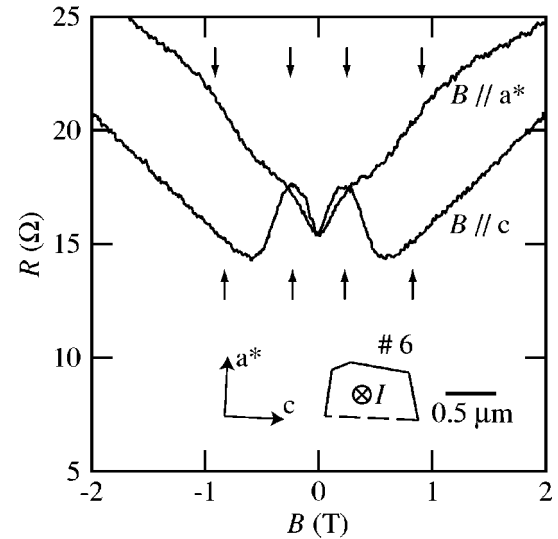


FIG. 4. The magnetoresistance of sample 6 at $T=1.72$ K. This sample has the narrowest width along the c axis. The upward arrows indicate the magnetic fields $B=0.55\hbar\sqrt{S_{a^*b}/\pi}/ed_{a^*}$ and $2.0\hbar\sqrt{S_{a^*b}/\pi}/ed_{a^*}$, while the downward arrows indicate $B=0.55\hbar\sqrt{S_{b^*c}/\pi}/ed_c$ and $2.0\hbar\sqrt{S_{b^*c}/\pi}/ed_c$.

path is shorter than the thickness d_{a^*} of the samples. McCarten *et al.*⁷ have estimated the bulk mean free path along the a^* axis, l_{a^*} to be $0.7\ \mu\text{m}$ at 4.2 K from the dependence of the $R(300\text{ K})/R(4.2\text{ K})$ on the crystal thickness in the range $0.1\text{--}10\ \mu\text{m}$, assuming diffuse scattering at the edges. This value of l_{a^*} explains the fact that the $R(B)$ curves of the samples with $d_{a^*}=1.9\ \mu\text{m}$ and $3.9\ \mu\text{m}$ do not show a maximum if the quality of our samples is similar to theirs. Note that the $R(B)$ curve of the crystal 2 ($d_{a^*}=0.60\ \mu\text{m}$) shows only a minimum, but no maximum, which implies that this crystal has a slightly shorter l_{a^*} .

Another fact consistent with l_{a^*} of $0.7\ \mu\text{m}$ is that the resistance peak for the sample having d_{a^*} of $0.49\ \mu\text{m}$ is obscured above about 12 K (Fig. 1). The bulk mean free path at 12 K is estimated to be about half of that at 4 K because the resistance of the thickest sample at 12 K is twice that at 4 K, and the carrier concentration hardly varies in this temperature range according to the literature.⁶ Thus, the reduction of the resistance peak with increasing temperature can be explained by decreasing l_{a^*} less than d_{a^*} .

The above discussion assumes that the surface scattering is completely diffuse. However, there may be a certain probability p of specular scattering, which would not contribute to the magnetoresistance peak. Actually, the data of McCarten *et al.* are also reasonably explained with p values up to 0.8.⁷ The estimation of l_{a^*} depends on the p value; $l_{a^*}\approx 10\ \mu\text{m}$ (at 4.2 K) for $p=0.8$. If the specular scattering is taken into consideration, the magnetoresistance peak should disappear when $l_{a^*}<d_{a^*}/(1-p)$. From this point of view, our data can be also roughly explained with p of 0.8 and l_{a^*} of $10\ \mu\text{m}$ at 4.2 K. A more reliable estimation of the p value needs an accurate determination of l_{a^*} from measurements on bulk crystals.

The resistance peak has not been observed in the field direction $B//a^*$ as shown in Fig. 2. We cannot definitively

account for this, but we presume that the bulk mean free path along the c axis, l_c , is smaller than $d_c/(1-p)$, where d_c is the width along the c axis. Figure 4 shows the magnetoresistance of the sample 6, which has the narrowest width d_c of $0.78\ \mu\text{m}$ along the c axis. The $R(B)$ curve of this sample for the field direction $B//a^*$ exceptionally exhibits a kink around $B \approx 0.3\ \text{T}$. This feature implies that there is a small surface-scattering effect, and therefore l_c is comparable to d_c in this sample, i. e., $\approx 1\ \mu\text{m}$, if $p=0$. From the data of the Hall and SdH measurements of the bulk NbSe_3 crystals, Ong⁶ has obtained the carrier mobility μ_c of $1.8\ \text{m}^2/\text{Vs}$ at $T=4.2\ \text{K}$ and a k_c of $1.6 \times 10^9\ \text{m}^{-1}$. These values correspond to an $l_c (= \hbar k_c \mu_c / e)$ of $1.9\ \mu\text{m}$, which is consistent with the above rough estimation. We should also note, however, that there appears to be another kink around $B \approx 1\ \text{T}$. Its origin is not clear at present.

The fact that the pocket of the Fermi surface has the shape of an ellipsoid elongated to the c axis may also make the resistance peak for $B//c$ distinct, and that for $B//a^*$ difficult to be observed. This is because in the field $B//c$, a larger

number of carriers have similar cyclotron radii, and hence suffer the surface scattering most strongly at similar magnetic fields. In fact, the amplitude of the SdH oscillation for $B//c$ is much larger than that for $B//a^*$, which can be understood in a similar way.

In summary, the transverse magnetoresistance curves of NbSe_3 crystals with a submicron thickness show a maximum at $B < 1\ \text{T}$, in addition to the SdH oscillation at $B \geq 2\ \text{T}$. The resistance maximum can be explained by semiclassical theories in terms of surface diffuse scattering of the normal carriers. Further studies are in progress to investigate the finite-size effect on magnetoresistance in the nonohmic regime $E > E_T$.

The authors wish to thank Y. Ootuka for kindly allowing the use of the SEM. This work was supported by a Grant-in-Aid for Scientific Research from the Ministry of Education, Culture, Sports, Science, and Technology (Grant No. 15073225).

¹For a review, see G. Grüner, *Rev. Mod. Phys.* **60**, 1129 (1988).

²P. Monceau, *Solid State Commun.* **24**, 331 (1977).

³R. M. Fleming, J. A. Polo, Jr., and R. V. Coleman, *Phys. Rev. B* **17**, 1634 (1978).

⁴P. Monceau and A. Briggs, *J. Phys. C* **11**, L465 (1978).

⁵N. Harrison, L. Balicas, J. S. Brooks, J. Sarrao, and Z. Fisk, *Phys. Rev. B* **61**, 14 299 (2000).

⁶N. P. Ong, *Phys. Rev. B* **18**, 5272 (1978).

⁷J. McCarten, D. A. DiCarlo, M. P. Maher, T. L. Adelman, and R. E. Thorne, *Phys. Rev. B* **46**, 4456 (1992); J. McCarten, M. Maher, T. L. Adelman, and R. E. Thorne, *Phys. Rev. Lett.* **63**, 2841 (1989).

⁸E. Slot, H. S. J. van der Zant, K. O'Neill, and R. E. Thorne, *Phys. Rev. B* **69**, 073105 (2004).

⁹O. C. Mantel, F. Chalin, C. Dekker, and H. S.J. van der Zant, Y. I. Latyshev, B. Pannetier, and P. Monceau, *Phys. Rev. Lett.* **84**, 538 (2000).

¹⁰J. C. Gill, *Solid State Commun.* **44**, 1041 (1982); M. P. Maher, T. L. Adelman, D. A. DiCarlo, J. P. McCarten, and R. E. Thorne, *Phys. Rev. B* **52** 13 850 (1995).

¹¹T. L. Adelman, S. V. Zaitsev-Zotov, and R. E. Thorne, *Phys. Rev. Lett.* **74**, 5264 (1995).

¹²D. MacDonald and K. Sarginson, *Proc. R. Soc. London* **203**, 223 (1950).

¹³E. Ditlefsen and J. Lothe, *Philos. Mag.* **14**, 759 (1966).

¹⁴K. Försvoll and I. Holwech, *Philos. Mag.* **9**, 435 (1964).

¹⁵T. J. Thornton, M. L. Roukes, A. Scherer, and B. P. Van de Gaag, *Phys. Rev. Lett.* **63**, 2128 (1989).